Calculation of vibrational branching ratios and hyperfine structure of ²⁴Mg¹⁹F and its suitability for laser cooling and magneto-optical trapping

Liang Xu, Yanning Yin, Bin Wei, Yong Xia, and Jianping Yin[*]

State Key Laboratory of Precision Spectroscopy and Department of Physics, East China Normal University, Shanghai 200062, China
(Received 5 November 2015; published 12 January 2016)

More recently, laser cooling of the diatomic radical magnesium monofluoride (²⁴Mg¹⁹F) is being experimentally preformed [Appl. Phys. Express **8**, 092701 (2015) and Opt. Express **22**, 28645 (2014)] and was also studied theoretically [Phys. Rev. A **91**, 042511 (2015)]. However, some important problems still remain unsolved, so, in our paper, we perform further theoretical study for the feasibility of laser cooling and trapping the ²⁴Mg¹⁹F molecule. At first, the highly diagonal Franck-Condon factors of the main transitions are verified by the closed-form approximation, Morse approximation, and Rydberg-Klein-Rees inversion methods, respectively. Afterwards, we investigate the lower $X\,^2\Sigma_{1/2}^+$ hyperfine manifolds using a quantum effective Hamiltonian approach and obtain the zero-field hyperfine spectrum with an accuracy of less than 30 kHz $\sim 5\,\mu$K compared with the experimental results, and then find out that one cooling beam and one or two repumping beams with their first-order sidebands are enough to implement an efficient laser slowing and cooling of ²⁴Mg¹⁹F. Meanwhile, we also calculate the accurate hyperfine structure magnetic g factors of the rotational state ($X\,^2\Sigma_{1/2}^+, N = 1$) and briefly discuss the influence of the external fields on the hyperfine structure of ²⁴Mg¹⁹F as well as its possibility of preparing three-dimensional magneto-optical trapping. Finally we give an explanation for the difference between the Stark and Zeeman effects from the perspective of parity and time reversal symmetry. Our study shows that, besides appropriate excitation wavelengths, the short lifetime for the first excited state $A\,^2\Pi_{1/2}$, and lighter mass, the ²⁴Mg¹⁹F radical could be a good candidate molecule amenable to laser cooling and magneto-optical trapping.

I. INTRODUCTION

Considerable progress has been achieved in laser cooling and magneto-optical trapping (MOT) of diatomic molecules, which should open the way to discover new physics and chemistry, such as the researches in the fields of cold chemistry, precision measurement, quantum simulation, and so forth [1–4]. In the past three decades, the laser cooling techniques to produce ultracold atoms [5–7] have made tremendous achievements, but usually they are difficult to be applied to neutral molecules due to their more complex internal structure and lack of a closed cooling transition cycle. Even so, besides some polar molecules (SrF, YO, CaF) [8–12] that have been demonstrated, there are some candidates suitable for laser cooling such as the ongoing YbF [13], BH [14], CaH [15], and even polyatomic SrOH [16]. For molecular complex structures, one of the main difficulties in laser cooling is to address various rotational and hyperfine levels of the electronic and vibrational (vibronic) states to provide the closure of the rotational ladder. Meanwhile, unlike atoms, controlling over vibrational transitions is particularly problematic because there is not a strict selection rule dominating the branching ratios for the decay of an electronic state into different vibrational states. The branching ratios of the vibrational levels are governed by the molecular Franck-Condon factors (FCFs); highly diagonal FCFs can reduce significantly the number of laser beams required experimentally to keep the molecule in a closed scattering cooling cycle and get repetitive momentum kicks. Generally speaking, any spontaneous decay from the electronically excited state can return inevitably to almost all of the vibrational states, several rotational states, and even many hyperfine structures (HFS) of the lower electronic state, but therein the rotational and HFS transitions still follow a strict angular momentum and parity selection rules fortunately.

Here the reason that we choose MgF to study its feasibility for laser cooling and MOT is because, in addition to its properties, some accurate spectroscopic constants for several electronic states are available. For example, the measurement of the absorption spectra of MgF molecules can be traced back to the 1930s, when the spectrum constants of the $X\,^2\Sigma_{1/2}^+$ and $A\,^2\Pi_{1/2}$ states were obtained from MgF absorption bands [17,18]. The first rotational structure of the 0-0 and 1-0 bands of the *A-X* system of MgF was measured and analyzed for $\lambda_{00} = 359.33$ nm and $\lambda_{10} = 368.76$ nm [19]; then the bands of the MgF molecule were found in the disk and spot spectra and as such are important in astrophysics [20]. In 1994, the pure rotational spectrum of the MgF molecules in the $X\,^2\Sigma_{1/2}^+$ state was used to analyze the rotational and hyperfine constants of this state [21,22]. In particular, the MgF molecule as a laser cooling candidate has the following characteristics: (i) a strong spontaneous radiation decay ($\Gamma = 2\pi \times 22$ MHz) due to its short lifetime of the excited state $A\,^2\Pi_{1/2}$ [23], and a relative large scattering force with lighter mass; (ii) the FCFs of the vibrational main transitions very close to unity; (iii) the simple and special HFS due to electron spin ($S = 1/2$), nuclear rotation, and nuclear spin ($I = 1/2$) interactions for the rotational $N = 1$ energy level of the ground state of MgF, and thus it is easy to match the hyperfine intervals of the state $X\,^2\Sigma_{1/2}^+$ with proper detuning by letting the cooling and repumping lasers pass through an electro-optic modulator (EOM) to split them into two frequency sidebands, respectively. More recently, laser cooling of MgF is being performed experimentally [24,25]

_____
[*]jpyin@phy.ecnu.edu.cn

and was theoretically studied [26]. However, some problems in theoretical calculations are still not well solved, such as the accurate FCFs, the relevant special HFS of MgF, and the influence of the external fields on the hyperfine structure in its MOT, and so on. So it would be interesting, worthwhile, and necessary to precisely calculate the vibrational branching ratios and the HFS of MgF and discuss its feasibility for laser cooling and MOT.

Usually, *ab initio* quantum chemical methods are used to calculate the potential energy curves of molecules, the vibrational transitions, and the FCFs in laser cooling of molecules, but they don't involve the hyperfine levels of molecules and their interaction with the external fields. Here we will perform the precise calculation of vibrational branching ratios for MgF by three different methods, use an quantum effective Hamiltonian approach to investigate the HFS of ^{24}Mg^{19}F, and discuss its feasibility for laser cooling and trapping. The paper is organized as follows. In Sec. II, the simple quantum description of the ^{24}Mg^{19}F molecule is introduced for the following calculations. In Sec. III, we calculate vibrational transition wavelengths and the FCFs between the ground state $X\,^2\Sigma_{1/2}^+$ and the first excited state $A\,^2\Pi_{1/2}$. Then the laser scheme for the closure of vibrational branchings is proposed. In Sec. IV, we introduce a quantum effective Hamiltonian for MgF and deduce its matrix representation, and then diagonalize it to obtain the zero-field energy spectrum of MgF in the lower manifolds. Next, the relevant energy levels and the experimental schemes are given for laser cooling and trapping this radical. Section V deals with the effects of applied electric and magnetic fields, that is, the Stark and Zeeman effects in MgF. We calculate the Stark and Zeeman shifts independently and get the accurate hyperfine magnetic g factors of the rotational state $(X\,^2\Sigma_{1/2}^+, N = 1)$ due to J mixing. From the perspective of parity and time reversal symmetry, we also give an explanation for the difference between the Stark and Zeeman effects in molecular system. Then we close in the final section, Sec. VI, with some main results and conclusions.

II. A SIMPLE QUANTUM DESCRIPTION FOR THE ^{24}Mg^{19}F RADICAL

Our model to describe the MgF molecule is composed of a magnesium nucleus, a fluorine nucleus, and 21 electrons, and the total kinetic energy operator is given by

$$\hat{T} = -\frac{\nabla_{Mg}^2}{2M_{Mg}} - \frac{\nabla_F^2}{2M_F} - \sum_{i=1}^{21}\frac{\nabla_i^2}{2m_e}, \qquad (1)$$

where M_{Mg}, M_F, and m_e are the masses of a magnesium nucleus, a fluorine nucleus, and an electron, respectively, and ∇_{Mg}, ∇_F, and ∇_i are the gradient operators with respect to the space coordinates of the magnesium nucleus R_{Mg}, fluorine nucleus R_F, and electron R_i. In this paper, we shall choose units such that $\hbar = 1$ unless quoting an energy in frequency units. Setting the center of mass of the magnesium nucleus and the fluorine nucleus as the origin of the coordinate system, that is, molecule-fixed coordinate system, we can rewrite the

kinetic energy operator as

$$\hat{T} = -\frac{\nabla_M^2}{2M} - \frac{1}{2mr^2}\frac{\partial}{\partial r}\left(r^2\frac{\partial}{\partial r}\right)$$
$$- \frac{1}{2mr^2}\left[\frac{1}{\sin\theta}\frac{\partial}{\partial\theta}\left(\sin\theta\frac{\partial}{\partial\theta}\right) + \frac{1}{\sin^2\theta}\frac{\partial^2}{\partial\phi^2}\right]$$
$$- \sum_{i=1}^{21}\frac{\nabla_i'^2}{2m_e} - \frac{1}{2(M_{Mg}+M_F)}\sum_{i,j=1}^{21}\nabla_i'\cdot\nabla_j', \qquad (2)$$

with the total mass of the molecule $M = M_{Mg} + M_F + 21m_e$ and the reduced mass of the two nuclei $m = M_{Mg}M_F/(M_{Mg} + M_F)$. The ∇_M and ∇_M' are gradient operators with respect to the coordinate of the center of mass of the molecule $R_M = (M_{Mg}R_{Mg} + M_FR_F + \sum_{i=1}^{21}m_eR_i)/M$ and the electronic coordinates r_i' is defined from the center of mass of the two nuclei, and r is the relative coordinate of the magnesium nucleus and fluorine nucleus in the polar coordinate (r,θ,ϕ). The first term in Eq. (2) describes the translational motion of the molecule, which will be neglected in our single molecular spectra study. The second and third terms represent vibration and rotation of the molecule, and the fourth and fifth terms are the kinetic operators of the electrons and the mass polarization term, respectively. Because of the large mass difference between electrons and nuclei, $m_e \ll M_{Mg}, M_F$, neglecting the mass polarization term is a very good approximation [27]. Thus, we will define the electronic Hamiltonian of the MgF molecule including the Coulomb repelling potential as

$$\hat{H}_{el} = -\sum_{i=1}^{21}\frac{\nabla_i'^2}{2m_e} + \frac{e^2}{4\pi\varepsilon_0}\left[\sum_{i<j}\frac{1}{r_{ij}} - \sum_{i=1}^{21}\left(\frac{Z_{Mg}}{r_{Mgi}} + \frac{Z_F}{r_{Fi}}\right)\right.$$
$$\left. + \frac{Z_{Mg}Z_F}{r}\right], \qquad (3)$$

where r_{ij} is the distance between electrons i and j, and r_{Mgi} (r_{Fi}) is the distance between the electron i and the magnesium nucleus (fluorine nucleus). The electric charges of an electron, the magnesium nucleus, and the fluorine nucleus are e, $Z_{Mg}e$, and Z_Fe, respectively, and ε_0 is the permittivity of vacuum. Then nuclear vibrational and rotational Hamiltonians of MgF are given by

$$\hat{H}_{vib} = -\frac{1}{2mr^2}\frac{\partial}{\partial r}\left(r^2\frac{\partial}{\partial r}\right), \qquad (4)$$

and

$$\hat{H}_{rot} = -\frac{1}{2mr^2}\left[\frac{1}{\sin\theta}\frac{\partial}{\partial\theta}\left(\sin\theta\frac{\partial}{\partial\theta}\right) + \frac{1}{\sin^2\theta}\frac{\partial^2}{\partial\phi^2}\right]. \qquad (5)$$

In principle, a full solution of the MgF molecular structure accounts for the motion of a magnesium nucleus, a fluorine nucleus, and 21 electrons. However, it is convincing that a typical diatomic molecule has the following relationship: $\Delta E_{vib}/\Delta E_{el} \approx \Delta E_{rot}/\Delta E_{vib} \approx (m_e/m)^{1/2} \approx 1/100$, where ΔE_{el}, ΔE_{vib}, and ΔE_{rot} are the energy separations between the ground state and the first excited state in electronic, vibrational, and rotational energy levels, respectively [27]. As we know, the molecule has very

TABLE I. Spectroscopic constants for the $X\,^2\Sigma_{1/2}^+$ and $A\,^2\Pi_{1/2}$ electronic states of MgF from the experimental data.

State	T_e (cm^{-1})	ω_e (cm^{-1})	$\chi_e\omega_e$ (cm^{-1})	R_e (Å)	B_e (cm^{-1})	Lifetime (ns)
$X\,^2\Sigma_{1/2}^+$	0	721.6 [19]	4.94 [19]	1.7500 [19]	0.5192 [19]	
		720.14 [29]	4.26 [29]	1.7499 [29]	0.5193 [29]	
$A\,^2\Pi_{1/2}$	27 816.1 [30]	740.12 [30]	3.97 [30]	1.7469 [30]	0.5210 [30]	7.16 [23]

complex intercouplings of degrees of freedom, whose energy differences are very large actually. Since there is very accurate and abundant spectroscopic information about this molecule, and the quantum chemistry method is very complicated and may be inaccurate, it is wise to take this radical as a vibratory rotor surrounded by electrons phenomenologically. Born and Oppenheimer [28] showed that the electrons move locally in an adiabatic potential generated by the slow motion of the nuclei, and hence a separable electronic-nuclear description with proper correction is an excellent approximation. So according to Eqs. (3)–(5), we can calculate the wavelengths of vibrational transitions and the FCFs between the $X\,^2\Sigma_{1/2}^+$ and $A\,^2\Pi_{1/2}$ states, which will be shown in the next section.

III. THE VIBRATIONAL TRANSITIONS AND FRANCK-CONDON FACTORS BETWEEN THE $X\,^2\Sigma_{1/2}^+$ AND $A\,^2\Pi_{1/2}$ STATES

Table I gives the electronic, vibrational, and rotational constants for MgF in the $X\,^2\Sigma_{1/2}^+$ and $A\,^2\Pi_{1/2}$ states. The total energy of a given state of a diatomic molecule is defined by the formula, $T = T_e + G + F$, where T_e, G, and F are the electronic energy, the vibrational energy, and the rotational energy, respectively. A transition frequency from the state $X\,^2\Sigma_{1/2}^+$ at energy T to the state $A\,^2\Pi_{1/2}$ at energy T' will be given (in cm^{-1}) by

$$\Delta T = T' - T = (T_e' - T_e) + (G' - G) + (F' - F). \quad (6)$$

Since, in general, the rotational energy change is much smaller than either the vibrational or electronic energy changes, we have after neglecting rotational energy,

$$\begin{aligned}\Delta T = T_e' &+ \big[\omega_e'\big(v' + \tfrac{1}{2}\big) - \omega_e'x_e'\big(v' + \tfrac{1}{2}\big)^2 \\ &+ \omega_e'y_e'\big(v' + \tfrac{1}{2}\big)^3 + \cdots\big] - \big[\omega_e\big(v + \tfrac{1}{2}\big) \\ &- \omega_e x_e\big(v + \tfrac{1}{2}\big)^2 + \omega_e y_e\big(v + \tfrac{1}{2}\big)^3 + \cdots\big], \quad (7)\end{aligned}$$

where v is the vibrational quantum number, and ω_e, $\omega_e x_e$, and $\omega_e y_e$ are the harmonic vibrational constant, and the first and second anharmonic corrections to the harmonic oscillator, respectively.

According to the molecular constants of MgF in Table I, we can directly calculate the vibrational transition wavelengths

(or frequencies), and the results are shown in Table II. It is clear that our calculated results are in good agreement with the experimental ones in Ref. [19]. Note that theoretically calculated and cited experimental values of the second and third wavelengths (λ_{10} and λ_{21}) in Table II of Ref. [26] are ones of the transition wavelengths (λ_{01} and λ_{12}) actually. So the three wavelengths (λ_{10}, λ_{21}, and λ_{31}) in Fig. 5 of Ref. [26] were labeled wrongly, because they violate a natural law, that is, the shorter the distance between the two energy levels is, the lower the transition frequency will be, and then the longer the transition wavelength should be, so we should have relationships of $\lambda_{31} > \lambda_{21}$ and $\lambda_{10} > \lambda_{00}$, not $\lambda_{31} < \lambda_{21}$ and $\lambda_{10} < \lambda_{00}$. In addition, our calculated precise wavelength values are very important for calculating FCFs and carrying out the forthcoming experiment.

These laser wavelengths ($\lambda_{00} = 359.3$ nm, $\lambda_{10} = 368.7$ nm, and $\lambda_{21} = 368.4$ nm) which will be used in laser cooling and trapping are in the UV region and can be generated by three continuous-wave (cw) frequency-doubled, frequency-stabilized, and single-frequency Ti:sapphire lasers or dye lasers, which have already been realized in our experiments with a narrow linewidth of 100–200 kHz and an extraordinary long-term frequency stability of 2.8 MHz [24,25].

The molecular FCFs are proportional to the square of the integral between the vibrational wave functions of the two states that are involved in the transition and represent the intensity of vibrational transitions for a molecular system, which imply the overlap of the vibrational wave functions for two different electronic states. According to the Franck-Condon principle, the electronic transition tends to occur vertically in the potential energy curve, which indicates therein almost invariable internuclear distance between the two states. Since the difference of equilibrium nuclear separation between the states $X\,^2\Sigma_{1/2}^+$ and $A\,^2\Pi_{1/2}$ of the MgF molecule is very small (about 0.0031 angstrom) [30], first we employ a closed-form approximation to estimate the relevant FCFs by the following formulas [31]:

$$f_{0v} = f_{v0} = \mu^v e^{-\mu}/v! \,(v \geqslant 0), \quad (8a)$$

$$f_{1v} = f_{v1} = \mu^{v-1} e^{-\mu}(u - v)/v! \,(v \geqslant 1), \quad (8b)$$

$$\cdots$$

TABLE II. The comparisons between theoretical and experimental results for the transition wavelengths from the $X\,^2\Sigma_{1/2}^+$ ($v = 0$, 1, and 2) to $A\,^2\Pi_{1/2}$ ($v' = 0$ and 1) states of MgF.

Transition wavelength	λ_{00} (cm^{-1})	λ_{10} (cm^{-1})	λ_{21} (cm^{-1})
Our calculation results	359.38	368.81	368.41
Experiment results	359.33 [19]	368.76 [19]	

TABLE III. The calculated FCFs $f_{v'v}$ of MgF by the methods of the closed-form estimation, Morse potential, and RKR inversion, respectively, in contrast with the results of other groups. The transitions happen between the $A\,^2\Pi_{1/2}(v')$ and $X\,^2\Sigma^+_{1/2}(v)$ states of MgF.

Method	f_{00} f_{10}	f_{01} f_{11}	f_{02} f_{12}	f_{03} f_{13}
The closed-form	0.9989	0.0011	0.0000	0.0000
approximation	0.0011	0.9967	0.0022	0.0000
Morse potential	0.9985	0.0013	0.0020	0.0000
	0.0013	0.9954	0.0027	0.0006
RKR inversion	0.9978	0.0022	0.0000	0.0000
	0.0022	0.9904	0.0074	0.0000
	0.986 [23]	0.014 [23]	0.000 [23]	0.000 [23]
Results of	0.9170 [26]	0.0790 [26]	0.0040 [26]	0.000 095 [26]
other groups	0.014 [23]	0.961 [23]	0.026 [23]	0.000 [23]
	0.0800 [26]	0.7760 [26]	0.1380 [26]	0.0058 [26]

where $\mu = S^2/2$, S is the transition parameter $(m\tilde{\omega})^{1/2}\Delta r_e/5.807$; m and v are the reduced mass of the diatomic molecule (in units of a.u.) and vibrational quantum number; $\tilde{\omega} = 2\omega_1\omega_2/(\omega_1 + \omega_2)$ describes an average of ω_e in the ground and excited states (in units of cm^{-1}); Δr_e is the difference between the internuclear distance r_e. The number 5.807 is equal to the value of $\sqrt{h/(4\pi^2 ca)}$ (in angstrom), h is Planck's constant (in J · s), c is the speed of light (in cm/s), and $a = 1$ amu (in kg). Afterwards, we calculate and analyze the FCFs by the methods of the Morse potential approximation [32,33] and the Rydberg-Klein-Rees (RKR) inversion [34], respectively, and the results are shown in Table III. We know that the MgF molecule is one of the molecules whose accurate spectroscopic constants for several electronic states are available, and the accuracy of the calculated FCFs depends critically on the potential energy curves employed. In the RKR method, the potential energy curves are constructed from the observed vibrational and rotational spectroscopic constants rather than by imposing an analytic form on the potential energy curves, so the RKR is more reliable. Meanwhile, when molecules are in the lower vibrational state, its real potential energy function tallies with the potential energy curve of Morse potential, so, the Morse approximation cannot only greatly reduce the complexity of the problem to some extent, but also ensure the calculation accuracy.

As shown in Table III, our three calculated results are basically consistent with each other and the ones in Ref. [23] and better than ones in Ref. [26] which may be due to the poor calculated accuracy of the potential energy curves, etc. We notice that by the Morse potential method the f_{02} is 0.0020, not 0.0000 by the other methods, which may originate from its slight aberrations for the vibrational state ($v = 2$). Based on the above calculated vibrational transition wavelengths $\lambda_{vv'}$ and the corresponding FCFs $f_{vv'}$, the laser scheme and spontaneous decays (red wavy lines) are depicted in Fig. 1. The use of the first excited state $A\,^2\Pi_{1/2}$ can ensure that no other electronic states participate in the cycles, meanwhile, we choose the transition $(v' = 0)\leftarrow(v = 0)$ (solid red lines) as a main cooling transition because of its favorable FCFs (f_{00}=0.9978). Because the off-diagonal transitions are suppressed intensely and the FCF f_{02} is less than 10^{-4}, we can efficiently cover the vibrational levels by using only two laser beams (one cooling laser $\lambda_{00} = 359.3$ nm and one repumping laser $\lambda_{00} = 368.7$ nm) and obtain more than 10^4 scattering photons, which is sufficient to stop and cool MgF in the buffer gas source. If another repumping laser ($\lambda_{10} = 368.4$ nm) is added, more transition cooling cycles for MgF can be obtained, which are more than that for SrF, YO, or CaF under the same condition, and even nearly similar to the case of laser cooling of Rb atoms. Thus we have achieved the closure of vibrational branching.
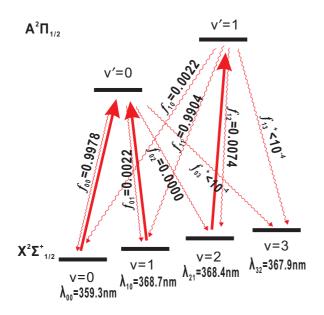

FIG. 1. The proposed scheme to create a quasicycling transition for laser cooling of MgF. Solid black lines indicate relevant electronic and vibrational structure in MgF. Solid upward lines indicate laser-driven transitions at the wavelengths $\lambda_{vv'}$. Solid wavy lines indicate spontaneous decays from the $A\,^2\Pi_{1/2}$ state with FCFs $f_{v'v}$ as shown.

IV. HYPERFINE STRUCTURE OF THE MgF RADICAL

In laser cooing of molecules, the lowest rovibrational levels of the ground electronic state play key roles to eliminate dark states and implement nearly closed optical transitions, which

was not studied in Ref. [26]. Meanwhile, it is important to take its HFS into account when we explore physics of cold molecules at micro-Kelvin (mK) temperatures and below [35]. For this, we will investigate HFS of the ground state $X\,^2\Sigma_{1/2}^+$ of the MgF radical by the method of matrix diagonalization which is more accurate than perturbation theory.

According to the above FCFs and the selection rule of the rotational levels, we only care about several lower rovibrational structures of the ground electronic state $X\,^2\Sigma_{1/2}^+$ of MgF in laser cooling and trapping. Throughout this paper, we assume that the vibrational state is a very small perturbation with respect to the electronic state, and nuclear rotation is also a very small perturbation with respect to vibration. In matrix mechanics, we take the vibronic energy as the diagonal elements in the constructed matrix.

J. H. Brown's book [27] told us that all kinds of inter-couplings of angular momenta in a molecular system can be given by the effective Hamiltonian which should act only on a subspace spanned by the vibronic states of the nonrelativistic kinetic, vibrational, and electrostatic Coulomb Hamiltonian, while reproducing the eigenenergy of the full Hamiltonian, for a typical diatomic molecule,

$$\hat{H}_{\text{eff}} = \hat{T}_0 + \hat{H}_{\text{SO}} + \hat{H}_{\text{SS}} + \hat{H}_{\text{SR}} + \hat{H}_{\text{Rot}} + \hat{H}_{\text{CD}} + \hat{H}_{\text{LD}} + \hat{H}_M + \hat{H}_Q, \tag{9}$$

where $\hat{T}_0$, $\hat{H}_{\text{SO}}$, $\hat{H}_{\text{SO}}$, $\hat{H}_{\text{SR}}$, $\hat{H}_{\text{Rot}}$, $\hat{H}_{\text{CD}}$, $\hat{H}_{\text{LD}}$, $\hat{H}_M$, and $\hat{H}_Q$ denote the vibronic energy, the electronic spin-orbit coupling, the electronic spin-spin coupling, the electronic spin-nuclear rotation coupling, the nuclear rigid rotation energy, the centrifugal distortion energy, Λ-doubling splitting, the magnetic hyperfine interactions, and the nuclear electric quadrupole interactions, respectively. In the $X\,^2\Sigma_{1/2}^+$ configuration of the MgF radical, the total spin $S = 1/2$ indicates that an unpaired valence electron forms an open shell structure, meanwhile, due to the projection component of the electronic orbital angular

momentum onto the internuclear z axis $\Lambda = 0$, we can remove the three terms $\hat{H}_{\text{SO}}$, $\hat{H}_{\text{SS}}$, and $\hat{H}_{\text{LD}}$ reasonably. Since we only consider the lowest vibronic state, it is convenient to take $\hat{T}_0 = 0$. For our isotope, $^{24}\text{Mg}^{19}\text{F}$, the nuclear spins of the magnesium nucleus and fluorine nucleus are $I_{\text{Mg}} = 1/2$ and $I_{\text{F}} = 1/2$, respectively, so the electric quadruple interactions in this diatomic radical is exactly zero. For the MgF radical, the $X\,^2\Sigma_{1/2}^+$ state can be described well by Hund's case (b), so an appropriate nonparity basis set in the absence of external field is given by $|\eta, \Lambda, N, S, J, I, F, M_F\rangle$, where the symbol η denotes all other quantum numbers not expressed explicitly, for example, electronic and vibrational ones, the letters N, J, I, and F are the total angular momentum excluding electron spin, the total angular momentum, the total nuclear spin, and the total angular momentum of molecule, respectively, and M_F is the projective component of F in a space-fixed Z direction and it is an important quantum number when we discuss the effects of the external magnetic or electric fields in the next section. As we all know, the spherical tensor method is very useful to describe the angular momenta and their interactions, both with each other and with applied external fields [36]. Here using Frosch and Foley constants [21,37], the effective Hamiltonian for the ground state of MgF can be expressed by

$$\hat{H}_0 = B_v \hat{N}^2 - D_v \hat{N}^4 + \gamma_v T^1(\hat{S}) T^1(\hat{N}) + b_{Fv} T^1(\hat{I}) T^1(\hat{S}) + c_v T_{q=0}^1(\hat{I}) T_{q=0}^1(\hat{S}) + C_{vN} T^1(\hat{I}) T^1(\hat{N}), \tag{10}$$

where B_v, D_v, γ_v, b_{Fv}, and c_v are the molecular rotational constant, the centrifugal distortion constant, the spin-rotational coupling constant, the Fermi contact interaction constant, and the dipole-dipole interaction constant, respectively. Note that $b_{Fv} = b_v + (1/3)c_v$, where b_v contains contributions from two different magnetic interactions, the Fermi contact and the electron-nuclear dipolar interaction. The constant C_{vN} is negligibly small generally but it is included in Eq. (10) just for completeness. Based on the Hund's case (b) basis, by using the total effective Hamiltonian and spherical tensor algebra, we can derive the following four

TABLE IV. The experimental spectral data and our theoretically calculated results and their comparisons for MgF. The first three columns are the permissible transitions between the rotational hyperfine levels of the $X\,^2\Sigma_{1/2}^+$ ($v = 0$) state. The fourth column is observational spectrum data in Ref. [21]. Our theoretical results are included in the fifth column and the differences between experimental data and theoretically calculated results are given in the last column.

$N \to N'$	$J \to J'$	$J \to J'$	v_{exp} (MHz)	v_{calc} (MHz)	$v_{\text{exp}} - v_{\text{calc}}$ (MHz)
$0 \to 1$	$1/2 \to 1/2$	$0 \to 1$	–	30 987.767	
	$1/2 \to 3/2$	$1 \to 2$	–	31 012.894	
$1 \to 2$	$1/2 \to 3/2$	$0 \to 1$	–	61 990.617	
	$3/2 \to 5/2$	$1 \to 2$	–	61 996.892	
$2 \to 3$	$3/2 \to 5/2$	$1 \to 2$	92 957.991	92 957.985	0.006
	$5/2 \to 7/2$	$2 \to 3$	92 991.900	92 991.882	0.018
$4 \to 5$	$7/2 \to 9/2$	$3 \to 4$	154 928.024	154 928.029	−0.005
	$9/2 \to 11/2$	$4 \to 5$	154 971.214	154 971.189	0.025
$5 \to 6$	$9/2 \to 11/2$	$4 \to 5$	185 909.344	185 909.372	−0.028
	$11/2 \to 13/2$	$5 \to 6$	185 954.406	185 954.433	−0.027
$6 \to 7$	$11/2 \to 13/2$	$5 \to 6$	216 886.282	216 886.297	−0.015
	$13/2 \to 15/2$	$6 \to 7$	216 932.633	216 932.632	0.001

matrix representations for the effective Hamiltonian,

$$\langle\eta',\Lambda',N',S,J',I,F',M_F'|B_v\hat{N}^2 - D_v\hat{N}^4|\eta,\Lambda,N,S,J,I,F,M_F\rangle = \delta_{\eta'\eta}\delta_{\Lambda'\Lambda}\delta_{N'N}\delta_{J'J}\delta_{F'F}\delta_{M_F'M_F}N(N+1)[B_v - D_vN(N+1)],$$
(11)

$$\langle\eta',\Lambda',N',S,J',I,F',M_F'|\gamma_v T^1(\hat{S})\cdot T^1(\hat{N})|\eta,\Lambda,N,S,J,I,F,M_F\rangle$$

$$= \delta_{\eta'\eta}\delta_{\Lambda'\Lambda}\delta_{N'N}\delta_{J'J}\delta_{F'F}\delta_{M_F'M_F}\gamma_v(-1)^{N+J+S}[S(S+1)(2S+1)]^{1/2}[N(N+1)(2N+1)]^{1/2}\begin{Bmatrix} S & N & J \\ N & S & 1 \end{Bmatrix},$$
(12)

$$\langle\eta',\Lambda',N',S,J',I,F',M_F'|b_{Fv}T^1(\hat{I})\cdot T^1(\hat{S})|\eta,\Lambda,N,S,J,I,F,M_F\rangle$$

$$= \delta_{\eta'\eta}\delta_{\Lambda'\Lambda}\delta_{N'N}\delta_{F'F}\delta_{M_F'M_F}b_{Fv}(-1)^{J'+F+I+J+N+1+S}[(2J'+1)(2J+1)]^{1/2}[S(S+1)(2S+1)I(I+1)(2I+1)]^{1/2}$$

$$\times \begin{Bmatrix} I & J' & F \\ J & I & 1 \end{Bmatrix}\begin{Bmatrix} J & S & N \\ S & J' & 1 \end{Bmatrix},$$
(13)

and

$$\langle\eta',\Lambda',N',S,J',I,F',M_F'|c_v T^1_{q=0}(\hat{I})T^1_{q=0}(\hat{S})|\eta,\Lambda,N,S,J,I,F,M_F\rangle$$

$$= \delta_{\eta'\eta}\delta_{\Lambda'\Lambda}\delta_{N'N}\delta_{F'F}\delta_{M_F'M_F}(-\sqrt{30}/3)c_v(-1)^{J'+F+I+N}[(2J'+1)(2J+1)]^{1/2}[S(S+1)(2S+1)I(I+1)(2I+1)]^{1/2}(2N+1)$$

$$\times \begin{pmatrix} N & 2 & N \\ 0 & 0 & 0 \end{pmatrix}\begin{Bmatrix} J & J' & 1 \\ N & N & 2 \\ S & S & 1 \end{Bmatrix}\begin{Bmatrix} I & J' & F \\ J & I & 1 \end{Bmatrix},$$
(14)

$$\langle\eta',\Lambda',N',S,J',I,F',M_F'|C_{vN}T^1(\hat{I})T^1(\hat{N})|\eta,\Lambda,N,S,J,I,F,M_F\rangle$$

$$= \delta_{\eta'\eta}\delta_{\Lambda'\Lambda}\delta_{N'N}\delta_{F'F}\delta_{M_F'M_F}C_{vN}(-1)^{2J+F'+I+N'+1+S}\sqrt{N(N+1)(2N+1)(2J'+1)(2J+1)}$$

$$\times \sqrt{I(I+1)(2I+1)}\begin{Bmatrix} I & J & F' \\ J' & I & 1 \end{Bmatrix}\begin{Bmatrix} N & J & S \\ J' & N' & 1 \end{Bmatrix}$$
(15)

where $\delta_{i'i}$, called the Kronecker delta function, is defined as having the properties that $\delta_{i'i} = 0$ for $i' \neq i$ and $\delta_{i'i} = 1$ for $i' = i$. We can obtain the state eigenvectors and the energy eigenvalues by diagonalizing the constructed matrix numerically, and then gain the transition frequencies between the rotational hyperfine levels (see Table IV). For these hyperfine states, the eigenvectors imply that as a result of the mixing between the J states in the same N, the good quantum number N and F have definite values but J does not, as shown in Table V.

The experimental observational spectral data and our theoretically calculated results for the $X\,^2\Sigma_{1/2}^+$ ($v = 0$) state of MgF are tabulated in Table IV. The fifth column denotes our calculated results, which are in perfect agreement with the observational transition frequencies (see the fourth column) between the higher rotational hyperfine levels [21] by an accuracy of less than 30 kHz $\sim 5\,\mu$K, so our theoretical

results and thus the methods are very reliable. The lower rotational transitions (especially for the $N = 1$ state) are very important for the closure of rotational branchings, but they have not yet been measured, so our calculated results for these lower levels have great significance for experimentally laser cooling and trapping the MgF molecules.

The closure of the rotational structures for MgF is plotted in Fig. 2. The MgF molecule has an unpaired electron spin $S = 1/2$ that splits the $X\,^2\Sigma_{1/2}^+$ ($N=1$) level into $J = N \pm S$ levels through spin-rotation interaction. The $X\,^2\Sigma_{1/2}^+$ state is well described by Hund's case (b) while the $A\,^2\Pi_{1/2}$ state is best described by Hund's case (a); the parity of the rotational ladder in the $X\,^2\Sigma_{1/2}^+$ states is given by $(-1)^N$, and for half-integral J in the $A\,^2\Pi_{1/2}$ state, levels with parities $(-1)^{J-1/2}$ or $(-1)^{J+1/2}$ are designated e or f, respectively [27]. We choose a ground state with $R = 1$

TABLE V. The g factors of the $X\,^2\Sigma_{1/2}^+$ ($v = 0, N = 1$) state of MgF. The first three columns include the nominal label, and the actual labels due to J mixing and J composition; the last two columns are the g factors without and with mixing of the states with the different J taken into account. The g factors below are valid for B fields which cause energy level shifts that are small compared to hyperfine structure splits.

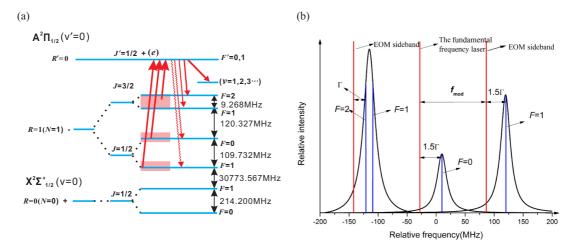| Nominal label	Actual label	J composition	g (without J mixing)	g (with J mixing)
$|J = 3/2, F = 2\rangle$	$|J = 3/2\rangle$	100% $J = 3/2$	0.50	0.50
$|J = 3/2, F = 1\rangle$	$0.6989|J = 3/2\rangle$	48.85% $J = 3/2$	0.83	0.71
	$+0.7152|J = 1/2\rangle$	51.15% $J = 1/2$		
$|J = 1/2, F = 0\rangle$	$|J = 1/2\rangle$	100% $J = 1/2$	0.00	0.00
$|J = 1/2, F = 1\rangle$	$-0.7152|J = 3/2\rangle$	51.15% $J = 3/2$	-0.33	-0.21
	$+0.6989|J = 1/2\rangle$	48.85% $J = 1/2$		

FIG. 2. The relevant energy-level structure, laser frequencies, spontaneous radiations, and fluorescence spectra for MgF. (a) Rotational branching is addressed by driving a $R' = 0 \leftarrow R = 1$ transition. Due to the even parity rotational state $J = 1/2(e)$ of the $A\,^2\Pi_{1/2}$, the angular momentum and parity selection rules allow a spontaneous decay only back to the odd parity rotational state $R = 1$ of $X\,^2\Sigma_{1/2}^+$. Here the vertical energies are not to scale. (b) The theoretically calculated molecular fluorescence spectra (black curved line) are shown with a natural linewidth Γ and its central frequencies (solid blue lines). To cover all sublevels of $X\,^2\Sigma_{1/2}^+(R = 1)$, the main cooling laser beam should be modulated by an EOM with a modulated frequency of about 115 MHz into two sidebands (solid red lines).

and drive a transition to an excited electronic state where $J' = 1/2(e)$, $R' = 0$ with a wavelength of $\lambda_{00} = 359.3$ nm. Due to strict parity and angular momentum selection rules of $\Delta R = 0, \pm 1$ for dipole transitions, molecules can only spontaneously decay back to the $R=1$ level of the ground state. However, ^{19}F has a nuclear spin $I = 1/2$ that splits J into $F = J \pm 1/2$ levels through magnetic and electric hyperfine interaction, and then the lower two rotational levels are split into two ($|J = 1/2, F = 0\rangle$ and $|J = 1/2, F = 1\rangle$) and four ($|J = 3/2, F = 1\rangle$, $|J = 3/2, F = 2\rangle$, $|J = 1/2, F = 0\rangle$, and $|J = 1/2, F = 1\rangle$) hyperfine energy levels, respectively. All these HFS sublevels of $N=1$ will be significantly populated in the whole cooling process. We can use an EOM with a modulated frequency of about 115 MHz to modulate the main cooling laser λ_{00} into two sidebands. Due to the small interval about 0.4Γ between $|J = 3/2, F = 1\rangle$ and $|J = 3/2, F = 2\rangle$, the two sidebands and fundamental frequency laser itself can cover the four hyperfine sublevels of the $X\,^2\Sigma_{1/2}^+$ ($v = 0, N = 1$) with a detuning about -1.5Γ, which also is required for the other two repumping lasers λ_{10} and λ_{21}. Here all dark states of the rotational and HFS branching will be eliminated perfectly and a quasiclosed transition cycle will be formed by only using one cooling laser and one or two repumping lasers for MgF molecules experimentally. In addition, the $A\,^2\Pi_{1/2}$ state has a short radiative lifetime ($\tau = 7.16$ ns) and a large spontaneous decay rate ($\Gamma = 2\pi \times 22$ MHz), so we can obtain a strong scattering force and realize an efficient Doppler laser slowing and cooling of MgF with a fast cooling rate.

V. THE INTERACTION BETWEEN EXTERNAL FIELDS AND HYPERFINE LEVELS OF MgF

In this section, we will add the effects of the external fields to Eq. (9) in order to study the MOT properties of MgF at cold or ultracold temperature. The manipulation of polar diatomic molecules with external field is also very necessary in some specific experiments, such as the Stark or Zeeman deceleration. The Hamiltonians of Stark and Zeeman interactions are given, respectively, by

$$\hat{H}_{\text{Stark}} = -T_{q=0}^1(\hat{\mu}_e)T_{p=0}^1(\hat{E}) = -\mu_e E_Z \cos\theta, \qquad (16)$$

and

$$\hat{H}_{\text{Zeeman}} = -T^1(\hat{\mu}_M)T_{p=0}^1(\hat{B})$$
$$= g_s\mu_B T^1(\hat{S})T_{p=0}^1(\hat{B}) + g_L\mu_L T^1(\hat{L})T_{p=0}^1(\hat{B})$$
$$- g_I\mu_N T^1(\hat{I})T_{p=0}^1(\hat{B}), \qquad (17)$$

where μ_e and μ_M are the molecular permanent electric dipole along the internuclear z axis ($q = 0$) [23] and the total magnetic dipole moment in a given state, respectively. Here the electron g factor is $g_s \approx 2.002$, the electron orbital g factor is $g_L \approx 1$, and the nuclear g factor is $g_I \approx 5.585$; μ_B is the Bohr magneton, and μ_N is the nuclear magneton. Since $\mu_N/\mu_B = 1/1836$ and $\Lambda = 0$, the first term in Eq. (17) is the most important. The subscripts p and q refer to the components of the space- and molecule-fixed coordinate system in spherical tensor. Then we can obtain two matrix representations as follows:

$$\langle \eta', \Lambda', N', S, J', I, F', M_F' | - T_{q=0}^1(\hat{\mu}_e)T_{p=0}^1(\hat{E})|\eta, \Lambda, N, S, J, I, F, M_F\rangle$$

$$= \delta_{\eta'\eta}\delta_{\Lambda'\Lambda}\delta_{M_F'M_F}\mu_e E_Z(-1)^{F'+F+1-M_F+J+I+J'+S+N}[(2N + 1)(2N' + 1)]^{1/2}[(2J + 1)(2J' + 1)(2F + 1)(2F' + 1)]^{1/2}$$

$$\times \begin{pmatrix} N & 1 & N' \\ 0 & 0 & 0 \end{pmatrix}\begin{Bmatrix} J & N & S \\ N' & J' & 1 \end{Bmatrix}\begin{Bmatrix} F & J & I \\ J' & F' & 1 \end{Bmatrix}\begin{pmatrix} F & 1 & F' \\ -M_F & 0 & M_F \end{pmatrix}, \qquad (18)$$
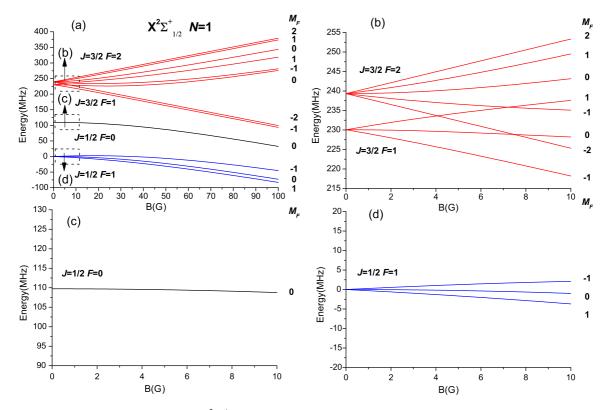
FIG. 3. (a) The Zeeman effect of MgF in the $X\,^2\Sigma_{1/2}^+$ ($v = 0, N = 1$) state, and the closeups of hyperfine structure as follows: (b) for the two levels $|J = 3/2, F = 2\rangle$ and $|J = 3/2, F = 1\rangle$ (red lines), (c) for the state $|J = 1/2, F = 0\rangle$ (black line), and (d) for the state $|J = 1/2, F = 1\rangle$ (blue lines). The energy levels are labeled by their M_F values at zero field.

and

$$\langle \eta', \Lambda', N', S, J', I, F', M_F' | g_s \mu_B T^1(\hat{S}) T_{p=0}^1(\hat{B}) | \eta, \Lambda, N, S, J, I, F, M_F \rangle$$

$$= \delta_{\eta'\eta} \delta_{\Lambda'\Lambda} \delta_{N'N} \delta_{M_F'M_F} g_s \mu_B B_Z (-1)^{F-M_F+F'+2J+I+N+S} [(2J+1)(2J'+1)S(S+1)]^{1/2}$$

$$\times [(2S+1)(2F+1)(2F'+1)]^{1/2} \begin{Bmatrix} J & S & N \\ S & J' & 1 \end{Bmatrix} \begin{Bmatrix} F & J & I \\ J' & F' & 1 \end{Bmatrix} \begin{pmatrix} F & 1 & F' \\ -M_F & 0 & M_F \end{pmatrix}. \tag{19}$$

From Eqs. (18) and (19), we can obtain the HFS Zeeman or Stark shifts of the $X\,^2\Sigma_{1/2}^+$ ($v = 0, N = 1$) state for MgF under static magnetic or electric fields as well as the g factors with taking the mixing of the states with the different J into account, and the results are plotted in Figs. 3 and 4 and Table V, respectively. It can be seen from Fig. 3(a) that each sublevel of the total angular momentum F will be shifted completely. In a typical MOT, the magnitude of magnetic field is about several Gauss. The two states $|J = 3/2, F = 1\rangle$ and $|J = 3/2, F = 2\rangle$ (red lines) have positive magnetic g factor $g_1 = 0.71$ and $g_2 = 0.50$ and they are split symmetrically and linearly into the eight magnetic sublevels, which are very favorable to realize the MOT. However, the $|J = 1/2, F = 1\rangle$ has a negative value $g = -0.21$ and the g factor of $|J = 1/2, F = 0\rangle$ is close to zero, and thus their magnetic sublevels have a small Zeeman shift, which would have a little contribution to the MOT, as shown in Figs. 3(b)–3(d). The rotational structure used in cooling and trapping MgF requires their cycling transitions to correspond to a type-II MOT system where $F' \leqslant F$ [10]. Due to a different sign g factors for the HFS of

$X\,^2\Sigma_{1/2}^+$ ($v = 0, N = 1$), we need a special optical polarization to match them experimentally [9,38,39].

It is worth noting in Figs. 3 and 4 that the Stark shift of each sublevel M_F in the electric field is entirely different from its Zeeman shift in the magnetic field; the Stark sublevels $|F, \pm M_F\rangle$ are exactly degenerate under the electronic field. This is because of the following reasons: First, as shown in Eq. (16) and (18), the $\cos\theta$ operator mixes Hund's case (b) basis vectors with the same M_F but N's which differ by ± 1 and thus have opposite parity. On the other hand, under parity inversion, the electric dipolar moment vector changes its direction, so the states coupled with each other due to Stark effect must be the opposite parities, and then the parity P, N, and J cease to be a good quantum number except for M_F. However, as shown in Eqs. (17) and (19), the S_Z operator couples Hund's case (b) basis functions with the same M_F and with the same N's (in the weak magnetic field) and thus have the same parity. On the other hand, the magnetic dipolar moment keeps unchanged under parity inversion, so the states coupled with each other due to the Zeeman effect
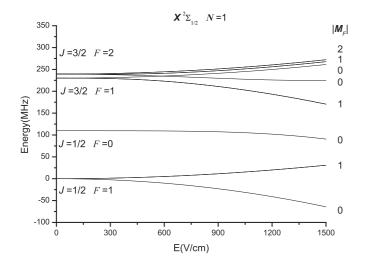
FIG. 4. The Zeeman effect of MgF in the $X\,^2\Sigma_{1/2}^+$ ($v = 0, N = 1$) state. There are always twofold degeneracies with $\pm M_F$ except for $M_F = 0$, so the energy levels are labeled by their $|M_F|$ values at zero field.

must be the same parities, and then the parity P and M_F are still good quantum numbers. Second, the electric dipolar moment vector commutes with the time reversal operator, but the magnetic dipolar moment vector does not have this property. So the effective Hamiltonian (including the Stark effect) remains unchanged under time reversal. Since the two states $|F, M_F\rangle$ and $|F, -M_F\rangle$ in the field E are time reversals of each other (forward and reverse) and the Hamiltonian is invariant under time reversal, the energy sublevels $|F, \pm M_F\rangle$ are exactly degenerate in the whole electric field. This situation will not occur in the magnetic field, because the Hamiltonian (including the Zeeman effect) in the magnetic field is changed under time reversal.

VI. CONCLUSIONS

In this paper, we have performed further theoretical study for the feasibility of laser cooling and trapping of the

^{24}Mg^{19}F radical. First, we calculated the vibrational transition wavelengths between the ground and first excited electronic states and their FCFs by three different methods, and found that our calculated results are in good agreement with the experimental data and more precise than the calculated results by the *ab initio* quantum chemistry method [26]. In particular, the highly diagonal FCFs indicate that two or three laser beams are enough to realize an efficient Doppler laser slowing and cooling of a buffer-gas cooled MgF molecular beam. Afterwards, using an effective Hamiltonian approach and irreducible tensor theory, we have calculated the hyperfine levels of the lower rotational states in the ground electric and vibrational state $X\,^2\Sigma_{1/2}^+$ ($v = 0, N = 1$) and obtained the hyperfine splitting spectrum with an accuracy of less than 30 kHz $\sim 5\,\mu$K compared with the experimental data, which is very important to eliminate the HFS dark states in the laser cooling and trapping of MgF. Finally, we have calculated the Zeeman and Stark shifts of the hyperfine levels of MgF and the exact HFS g factors of the lower rotational states in the ground state, and briefly discussed the feasibility of preparing MOT of MgF. According to parity and time reversal symmetry, we also explained the difference between the Stark and Zeeman effects in the molecular system. Our study shows that the MgF radical has available pumping wavelengths, highly diagonal FCFs, small and special splits of HFS, and a short lifetime of the excited state, which together make it a better candidate molecule than SrF and CaF for laser cooing and trapping (MOT) in principle.

[1] D. DeMille, Quantum Computation with Trapped Polar Molecules, Phys. Rev. Lett. **88**, 067901 (2002).

[2] J. Doyle, B. Friedrich, R. V. Krems, and F. Masnou-Seeuws, Editorial: Quo vadis, cold molecules? Eur. Phys. J. D **31**, 149 (2004).

[3] L. D. Carr, D. DeMille, R. V. Krems, and J. Ye, Cold and ultracold molecules: Science, technology and applications, New J. Phys. **11**, 055049 (2009).

[4] D. S. Jin and J. Ye, Introduction to ultracold molecules: New frontiers in quantum and chemical physics, Chem. Rev. **112**, 4801 (2012).

[5] S. Chu, The manipulation of neutral particles, Rev. Mod. Phys. **70**, 685 (1998).

[6] C. N. Cohen-Tannoudji, Manipulating atoms with photons, Rev. Mod. Phys. **70**, 707 (1998).

[7] W. D. Phillips, Laser cooling and trapping of neutral atoms, Rev. Mod. Phys. **70**, 721 (1998).

[8] E. S. Shuman, J. F. Barry, and D. DeMille, Laser cooling of a diatomic molecule, Nature (London) **467**, 820 (2010).

[9] J. F. Barry, D. J. McCarron, E. B. Norrgard, M. H. Steinecker, and D. DeMille, Magneto-optical trapping of a diatomic molecule, Nature (London) **512**, 286 (2014).

[10] M. T. Hummon, M. Yeo, B. K. Stuhl, A. L. Collopy, Y. Xia, and J. Ye, 2D Magneto-Optical Trapping of Diatomic Molecules, Phys. Rev. Lett. **110**, 143001 (2013).

[11] T. E. Wall, J. F. Kanem, J. J. Hudson, B. E. Sauer, D. Cho, M. G. Boshier, E. A. Hinds, and M. R. Tarbutt, Lifetime of the $A(v' = 0)$ state and Franck-Condon factor of the A-X(0-0) transition of CaF measured by the saturation of laser-induced fluorescence, Phys. Rev. A **78**, 062509 (2008).

[12] V. Zhelyazkova, A. Cournol, T. E. Wall, A. Matsushima, J. J. Hudson, E. A. Hinds, M. R. Tarbutt, and B. E. Sauer, Laser cooling and slowing of CaF molecules, Phys. Rev. A **89**, 053416 (2014).

[13] I. J. Smallman, F. Wang, T. C. Steimle, M. R. Tarbutt, and E. A. Hinds, Radiative branching ratios for excited states of ^{174}YbF: Application to laser cooling, J. Mol. Spectrosc. **300**, 3 (2014).

[14] R. J. Hendricks, D. A. Holland, S. Truppe, B. E. Sauer, and M. R. Tarbutt, Vibrational branching ratios and hyperfine structure of ^{11}BH and its suitability for laser cooling, Front. Phys. **2**, 51 (2014).

[15] J. Velasquez III and M. D. Di Rosa, Laser Cooling the Diatomic Molecule CaH, Proceeding of 69th International Symposium on Molecular Spectroscopy (2014).

[16] I. Kozyryev, L. Baum, K. Matsuda, P. Olson, B. Hemmerling and J. M. Doyle, Collisional relaxation of vibrational states of SrOH with He at 2K, New J. Phys. **17**, 045003 (2015).

[17] F. A. Jenkins and R. Grinfeld, The Spectrum of MgF, Phys. Rev. **45**, 229 (1934).

[18] C. A. Fowler Jr., New absorption spectra of the alkaline earth fluorides, Phys. Rev. **59**, 645 (1941).

[19] R. F. Brarrow and J. R. Beale, Rotational analysis of electronic bands of gaseous MgF, Proc. Phys. Soc. (London) **91**, 483 (1967).

[20] T. V. Ramakrishna Rao and S. V. J. Lakshman, The true potential energy curves, r-centroids and Franck-Condon factors of the bands of the $B^2\Sigma^+$-$X^2\Sigma^+$ system of MgF, Physica (Amsterdam) **46**, 609 (1970).

[21] M. A. Anderson, M. D. Allen, and L. M. Ziurys, Millimeter and submillimeter rest frequencies for the MgF radical, Astrophys. J. **425**, L53 (1994).

[22] M. A. Anderson, M. D. Allen, and L. M. Ziurys, Millimeter-wave spectroscopy of MgF: Structure and bonding in alkaline-earth monofluoride radicals, J. Chem. Phys. **100**, 824 (1994).

[23] M. Pelegrini, C. S. Vivacqua, O. Roberto-Neto, F. R. Ornellas, and F. B. C. Machado, Radiative transition probabilities and lifetimes for the band system $A^2\Pi$-$X^2\Sigma^+$ of the isovalent molecules BeF, MgF. and CaF, Braz. J. Phys. **35**, 950 (2005).

[24] D. P. Dai, Y. Xia, Y. N. Yin, X. X. Yang, Y. F. Fang, X. J. Li, and J. P. Yin, A linewidth-narrowed and frequency-stabilized dye laser for application in laser cooling of molecules, Opt. Express **22**, 28645 (2014).

[25] Y. N. Yin, Y. Xia, X. J. Li, X. X. Yang, S. P. Xu, and J. P. Yin, Narrow-linewidth and stable-frequency light source for laser cooling of magnesium fluoride molecules, Appl. Phys. Express **8**, 092701 (2015).

[26] S. Y. Kang, Y. F. Gao, F. G. Kuang, T. Gao, J. G. Du, and G. Jiang, Theoretical study of laser cooling of magnesium monofluoride using *ab initio* methods, Phys. Rev. A **91**, 042511 (2015).

[27] J. H. Brown and A. Carrington, *Rotational Spectroscopy of Diatomic Molecules* (Cambridge University Press, Cambridge, 2012).

[28] M. Born and R. Oppenheimer, Zur quantentheorie der molekeln, Ann. Phys. **389**, 457 (1927).

[29] B. E. Barber, K.-Q. Zhang, B. Guo, and P. F. Bernath, Vibration-rotation emission spectrum of MgF, J. Mol. Spectrosc. **169**, 583 (1995).

[30] K. P. Huber and G. Herzberg, *Molecular Spectra and Molecular Structure IV: Constants of Diatomic Molecules* (Van Rostrand-Reinhold, New York, 2005).

[31] R. W. Nicholls, Franck-Condon factor formulae for astrophysical and other molecules, J. Suppl. Ser. **47**, 279 (1981).

[32] X. S. Liu, X. Y. Liu, Z. Y. Zhou, P. Z. Ding, and S. F. Pan, Numerical solution of one-dimensional time-independent schrödinger equation by using symplectic schemes, Int. J. Quantum Chem. **79**, 343 (2000).

[33] V. I. Arnold, *Mathematical Method of Classical Mechanics* (Van Rostrand-Reinhold, New York, 1978).

[34] R. J. Le Roy, Level 8.0, *A Computer Program for Solving the Radial Schrodinger Equation for Bound and Quasibound Levels*, Chemical Physics Research Report No. 663 (University of Waterloo, Waterloo, Ontario, 2007).

[35] C. C. Ticknor, Ph.D thesis, Controlling cold collisions of polar molecules with external field, University of Colorado, 2005.

[36] R. N. Zare, *Angular Momentum: Understanding Spatial Aspects in Chemistry and Physics* (Wiley, New York, 1988).

[37] R. A. Frosch and H. M. Foley, Magnetic hyperfine structure of diatomical molecules, Phys. Rev. **88**, 1337 (1952).

[38] M. R. Tarbutt, Magneto-optical trapping forces for atoms and molecules with complex level structures, New J. Phys. **17**, 015007 (2015).

[39] D. J. McCarron, E. B. Norrgard, M. H. Steinecker, and D. DeMille, Improved magneto-optical trapping of a diatomic molecule, New J. Phys. **17**, 035014 (2015).